



Research article

A new 4D hyperchaotic system and its control

Ning Cui and Junhong Li*

School of Mathematics and Statistics, Hanshan Normal University, Chaozhou, Guangdong 521041, China

* **Correspondence:** Email: jhli2011@163.com.

Abstract: This paper presents a new four-dimensional (4D) hyperchaotic system by introducing a linear controller to 3D chaotic Qi system. Based on theoretical analysis and numerical simulations, the dynamical behaviors of the new system are studied including dissipativity and invariance, equilibria and their stability, quasi-periodic orbits, chaotic and hyperchaotic attractors. In addition, the Hopf bifurcation at the zero equilibrium point and hyperchaos control of the system are investigated. The numerical simulations, including phase diagram, Lyapunov exponent spectrum, bifurcations and Poincaré maps are carried out in order to analyze and verify the complex phenomena of the 4D hyperchaotic system.

Keywords: hyperchaos; Lyapunov exponents; bifurcation; hyperchaos control

Mathematics Subject Classification: 34K18, 65P20

1. Introduction

Hyperchaotic system is characterized as a chaotic system with at least two Lyapunov exponents [1] and the minimal dimension of the phase space that embeds the hyperchaotic attractor should be more than three. These imply that hyperchaos has more complex, dynamical phenomena than chaos. Compared to chaos, hyperchaos has greater potential applications due to its higher dimensions, stronger randomness and unpredictability such as secure communications [2, 3], nonlinear circuits [4, 5], lasers [6, 7], et al. In addition, as far as we know, the complexity of the hyperchaotic system dynamics has not been completely mastered by researchers until now. There are few studies on rich dynamical behaviors of hyperchaotic systems. Furthermore, it is difficult to find effective ways to analysis and study the complex dynamical phenomena of the high-dimensional hyperchaotic systems. Thus, it is necessary to formulate new high-dimensional hyperchaotic systems and to further investigate the properties of hyperchaos. Meanwhile, there have been many hyperchaotic systems presented. By adding a controlled variable to the Lorenz system, a hyperchaotic system was obtained in [8, 9]. [10]

presented a 4D generalised Lorenz hyperchaotic system by introducing a linear state feedback control to the first state equation of a generalised Lorenz system. [11] constructed a memristive hyperchaotic system by adding the flux-controlled memristor to an extended jerk system. Based on Chua's electrical circuit, [12] constructed a hyperchaotic system by introducing an additional inductor and [13] designed a hyperchaotic circuit system by replacing the non-linear element with an experimentally realizable memristor. Furthermore, there are also some scholars who constructed their own hyperchaotic systems [14, 15].

In [16], a chaotic system was introduced

$$\begin{cases} \dot{u} = a(v - u) + evw, \\ \dot{v} = cu + dv - uw, \\ \dot{w} = -bw + uv, \end{cases} \quad (1.1)$$

where $(u, v, w)^T \in \mathbb{R}^3$ is the state vector. a, b, c are positive real parameters and $c \in R$. When $(a, b, c, d, e) = (14, 43, -1, 16, 4)$, system (1.1) has four-wing chaotic attractor. The chaotic system was different from the Lorenz system family and some scholars have investigated the system including mechanical analysis, chaos control, energy cycle, bound and constructing 4D hyperchaotic systems [17–22]. In this work, we introduce a new 4D hyperchaotic system by adding a linear controller to system (1.1) as:

$$\begin{cases} \dot{u} = a(v - u) + evw, \\ \dot{v} = cu + dv - uw + mp, \\ \dot{w} = -bw + uv, \\ \dot{p} = -ku - kv, \end{cases} \quad (1.2)$$

where a, b, c, d, e, m, k are positive real parameters and $c \in R$.

The rest of this paper is organized as follows: in the second section, dissipativity and invariance, equilibria and their stability of system (1.2) are discussed. In addition, the complex dynamical behaviors such as quasi-periodicity, chaos and hyperchaos are numerically verified by Lyapunov exponents, bifurcation and Poincaré maps. In the third section, the Hopf bifurcation at the zero equilibrium point of system (1.2) is investigated. In addition, two examples are given to test and verify the theoretical results. The new system always has two unstable nonzero equilibrium points and has rich dynamical behaviors under different system parameters. Thus, the new 4D system may be more useful in some fields such as image encryption, secure communication. In the fourth section, the hyperchaos control is studied. The results show that the linear feedback control method can achieve a good control effect by selecting appropriate feedback coefficients. In the last section, the conclusions are summarized.

2. Dynamical analysis

2.1. Dissipativity and invariance

We can see that system (1.2) is invariant for the coordinate transformation

$$(u, v, w, p) \rightarrow (-u, -v, w, -p).$$

Then, the nonzero equilibria of (1.2) is symmetric with respect to w axis. The divergence of (1.2) is

$$\nabla W = \frac{\partial \dot{u}}{\partial u} + \frac{\partial \dot{v}}{\partial v} + \frac{\partial \dot{w}}{\partial w} + \frac{\partial \dot{p}}{\partial p} = -(a + b - d).$$

By Liouville's theorem, we get

$$\frac{dV(t)}{dt} = \int_{\Sigma(t)} (d - a - b) du dv dw dp = -(a + b - d)V(t),$$

where $\Sigma(t)$ is any region in R^4 with smooth boundary and $\Sigma(t) = \Sigma_0(t)$, $\Sigma_0(t)$ denotes the flow of W and the hypervolume of $\Sigma(t)$ is $V(t)$. For initial volume $V(0)$, by integrating the equation, we have

$$V(t) = \exp(-(a + b - d)t)V(0), (\forall t \geq 0).$$

Hence, system (1.2) is dissipative if and only if $a + b - d > 0$. It shows that each volume containing the system trajectories shrinks to zero as $t \rightarrow \infty$ at an exponential rate $-(a + b - d)$. There exists an attractor in system (1.2).

2.2. Equilibria

By computations, system (1.2) has three equilibrium points

$$E_0 = (0, 0, 0, 0)$$

and

$$E_1 = \left(\sqrt{\frac{2ab}{e}}, -\sqrt{\frac{2ab}{e}}, -\frac{2a}{e}, \frac{\sqrt{2eab}(de - ce - 2ad)}{e^2m} \right),$$

$$E_2 = \left(-\sqrt{\frac{2ab}{e}}, \sqrt{\frac{2ab}{e}}, -\frac{2a}{e}, -\frac{\sqrt{2eab}(de - ce - 2ad)}{e^2m} \right).$$

The characteristic equation of Jacobian matrix at E_0 is

$$(\lambda + b)[\lambda^3 + (a - d)\lambda^2 + (km - ac - da)\lambda + 2akm]. \quad (2.1)$$

According to Routh-Hurwitz criterion [23], the real parts of eigenvalues are negative if and only if

$$a > d, ad^2 + (ac - a^2 - km)d > a^2c + akm.$$

The Jacobian matrices at E_1 and E_2 have the same characteristic equation, i.e.,

$$\lambda^4 + e(a + b - d)\lambda^3 + a_2\lambda^2 + a_1\lambda - 4abkm,$$

where

$$a_2 = km - ab + ac - ad - bd + \frac{2a^2d + 2abd}{e}, \quad a_1 = (3ac + ad + km)b + \frac{10dba^2}{e}.$$

Note $4abkm > 0$, then the two nonzero equilibrium points are unstable.

2.3. Lyapunov exponents and Poincaré maps

In this subsection, some properties of the system (1.2) are discussed and the simulation results are further obtained by using numerical methods. Firstly, fix $a = 15$, $b = 43$, $c = 1$, $d = 16$, $e = 5$, $m = 5$ and varies k . Figure 1 indicates the Lyapunov exponent spectrum of system (1.2) with respect to $k \in [1.5, 5.5]$ and the corresponding bifurcation diagram is given in Figure 2. From Figures 1 and 2, the complex dynamical behaviors of system (1.2) can be clearly observed. Figure 1 indicates that system (1.2) has hyperchaotic attractors with two positive Lyapunov exponents when k varies in $[1.5, 5.5]$. When $(a, b, c, d, e, m, k) = (15, 43, 1, 16, 5, 5, 2)$, system (1.2) has three unstable equilibrium points

$$E_0 = (0, 0, 0, 0), E_1 = (-16.062, 16.062, -6, 260.210), E_2 = (16.062, -16.062, -6, -260.210).$$

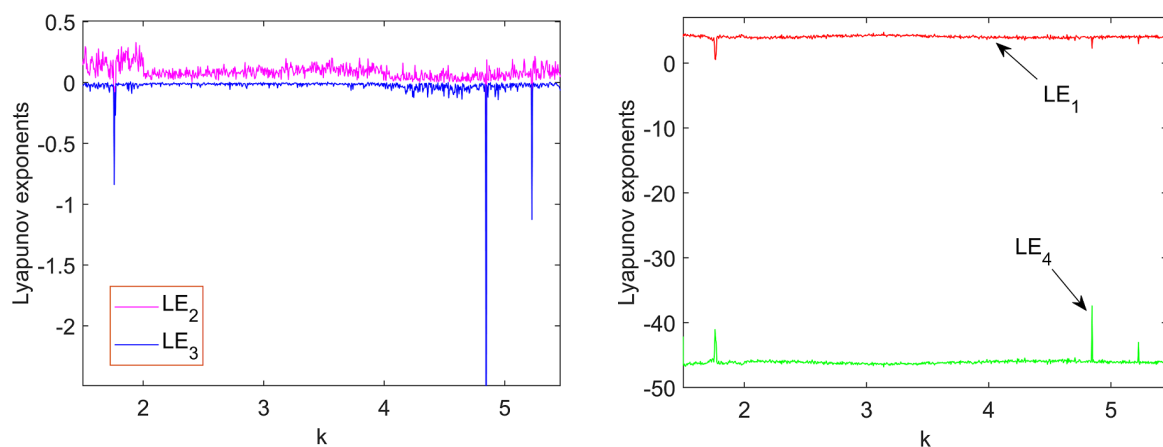


Figure 1. Lyapunov exponent spectrum of (1.2) with $k \in [1.5, 5.5]$.

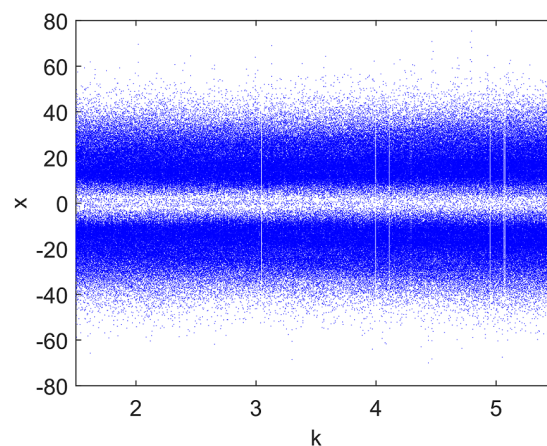


Figure 2. Bifurcation diagram of x .

The first and the second Lyapunov exponents are 4.273 and 0.092, these imply that system (1.2) is hyperchaotic. Figure 3 shows the (u, v, w, p) 4D surface of section and the location of the consequents is given in the (u, v, w) subspace and are colored according to their p value. Figure 4 shows the Poincaré maps on $u - p$ plane and $w - p$ plane, respectively.

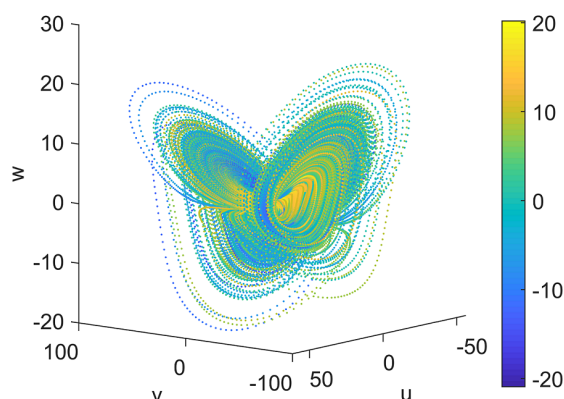


Figure 3. Projection on (u, v, w, p) .

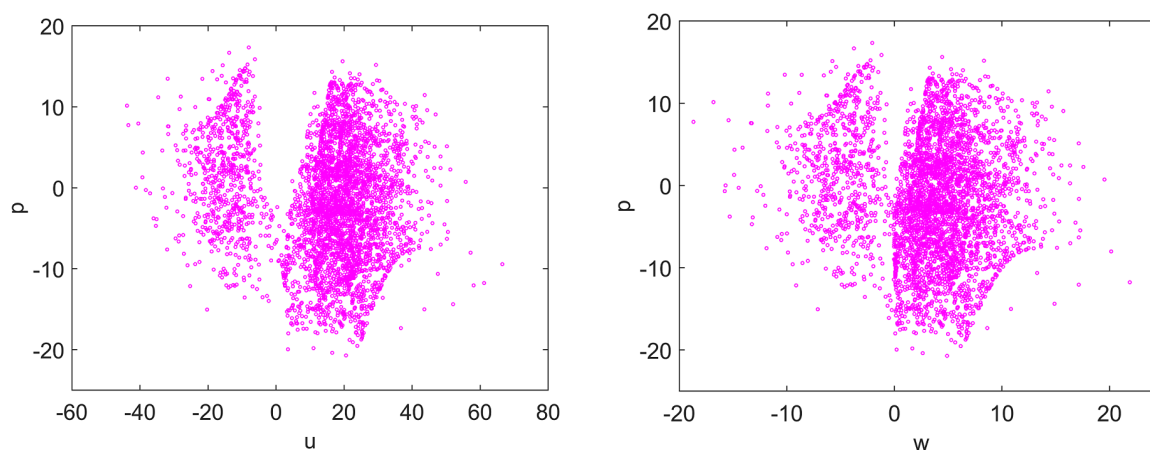


Figure 4. Poincaré maps on the $u - p$ plane and $w - p$ plane.

Assume $b = 43$, $a = 15$, $c = 1$, $e = 5$, $k = 5$, $d = 16$, the different Lyapunov exponents and dynamical properties with different values of parameter m are given in Table 1. As we can see in Table 1, system (1.2) is hyperchaotic with different m values. When $b = 43$, $a = 15$, $c = 1$, $e = 5$, $k = 5$, $d = 16$, $m = 0.5$, the hyperchaotic attractor on (v, u, w, p) space is depicted in Figure 5, the location of the consequents is given in the (v, u, w) subspace and are colored according to their p value. Figure 6 shows the Poincaré map on $v - w$ plane. It shows that system (1.2) has different hyperchaotic phenomena under different parameter values.

Table 1. Lyapunov exponents of (1.2) with $(b, a, c, e, k, d) = (43, 15, 1, 5, 5, 16)$.

| m | LE_1 | LE_2 | LE_3 | LE_4 | Dynamics |
|-----|--------|--------|--------|---------|------------|
| 0.5 | 3.827 | 0.036 | -0.000 | -45.862 | Hyperchaos |
| 1 | 3.901 | 0.052 | 0.000 | -45.953 | Hyperchaos |
| 1.5 | 3.943 | 0.081 | -0.000 | -46.022 | Hyperchaos |
| 2 | 4.277 | 0.091 | -0.000 | -46.364 | Hyperchaos |
| 2.5 | 4.221 | 0.106 | -0.000 | -46.325 | Hyperchaos |
| 3 | 3.976 | 0.075 | -0.000 | -46.040 | Hyperchaos |

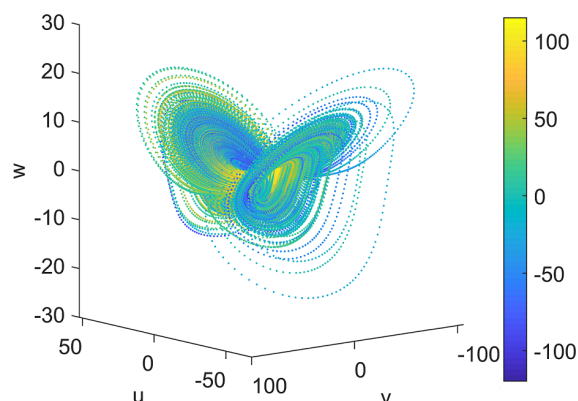


Figure 5. Projection on (v, u, w, p) .

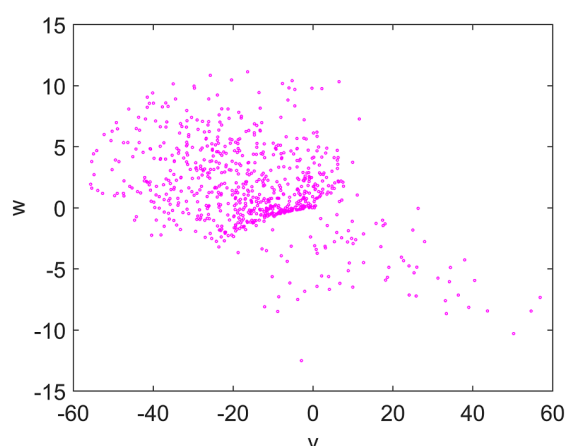


Figure 6. Poincaré map on $v - w$ plane.

When $(b, a, c, d, e, m, k) = (45, 15, 2, 15.9, 5, 0.1, 0.1)$, (1.2) has three unstable equilibrium points

$$E_0 = (0, 0, 0, 0),$$

$$E_1 = (-16.431, 16.431, -6, 13391.816),$$

$$E_2 = (16.431, -16.431, -6, -13391.816).$$

The Lyapunov exponents are $LE_1 = 1.979$, $LE_2 = 0.000$, $LE_3 = -0.002$, $LE_4 = -46.077$, system (1.2) is chaotic. Figure 7 shows the (v, u, w, p) 4D surface of section and the location of the consequents is given in the (v, u, w) subspace and are colored according to their p value. When $(b, a, c, d, e, m, k) = (45, 15, 2, 15.01, 5, 0.1, 0.1)$, system (1.2) has three unstable equilibrium points

$$O = (0, 0, 0, 0),$$

$$E_1 = (-16.431, 16.431, -6, 12660.606),$$

$$E_2 = (16.431, -16.431, -6, -12660.606).$$

The Lyapunov exponents are $LE_1 = -0.000$, $LE_2 = -0.000$, $LE_3 = -0.020$, $LE_4 = -44.963$, system (1.2) has quasi-periodic orbit. The (v, u, w, p) 4D surface of section is depicted in Figure 8, the location of the consequents is given in the (v, u, w) subspace and are colored according to their p value.

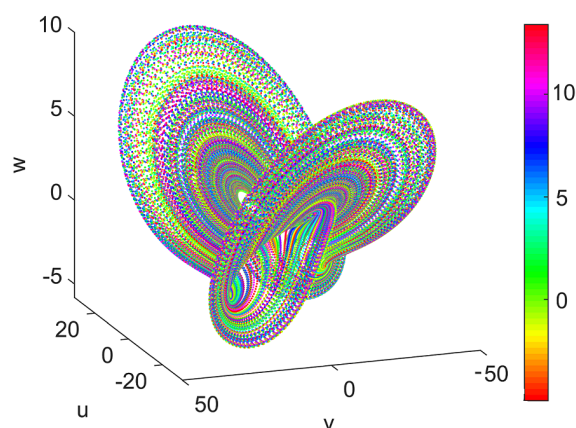


Figure 7. Projection on (v, u, w, p) .

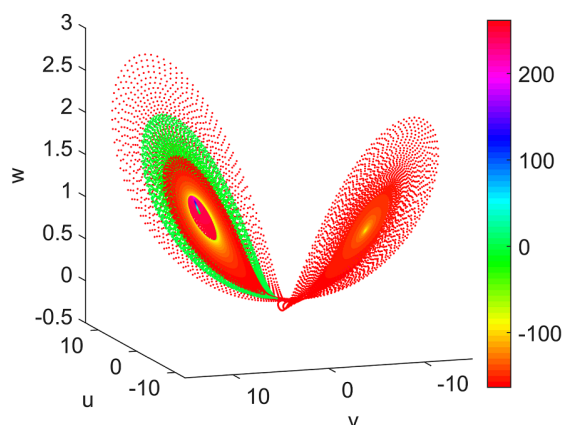


Figure 8. Projection on (v, u, w, p) .

When $(b, a, c, d, e, m, k) = (45, 15, 2, 15.1, 5, 0.1, 0.1)$, system (1.2) has three unstable equilibrium points

$$E_0 = (0, 0, 0, 0),$$

$$E_1 = (-16.431, 16.431, -6, 12734.549),$$

$$E_2 = (16.431, -16.431, -6, -12734.549).$$

The Lyapunov exponents are $LE_1 = 0.066$, $LE_2 = 0.000$, $LE_3 = -0.005$, $LE_4 = -44.961$, system (1.2) is chaotic. When $(b, a, c, d, e, m, k) = (45, 15, 2, 15.04, 5, 0.1, 0.1)$, system (1.2) has three unstable equilibrium points

$$E_0 = (0, 0, 0, 0),$$

$$E_1 = (-16.431, 16.431, -6, 12685.254),$$

$$E_2 = (16.431, -16.431, -6, -12685.254).$$

The Lyapunov exponents are $LE_1 = 0.000$, $LE_2 = -0.000$, $LE_3 = -0.010$, $LE_4 = -44.948$, system (1.2) is quasi-periodic. Similar to Figures 7 and 8, the corresponding chaotic attractor and quasi-periodic orbit on (v, u, w, p) space are given in Figures 9 and 10, respectively. Overall, the results

indicate that system (1.2) has rich and complex dynamical behaviors including hyperchaos, chaos and quasi-periodicity with different parameters.

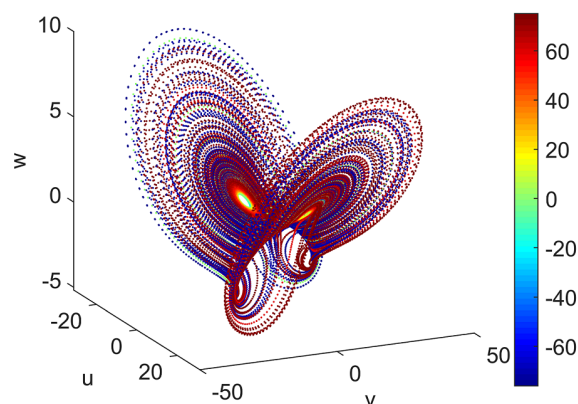


Figure 9. Projection on (v, u, w, p) .

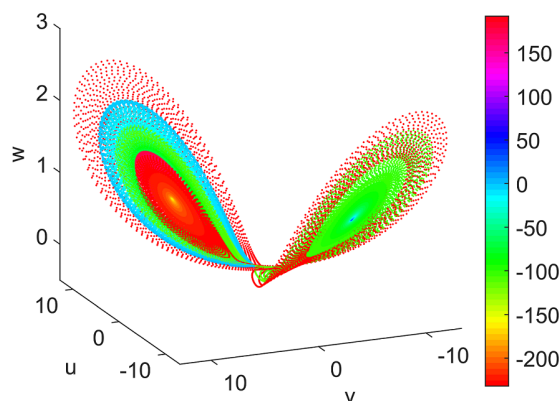


Figure 10. Projection on (v, u, w, p) .

3. Hopf bifurcation

Theorem 3.1. Suppose that $a - d > 0$ and $c + d < 0$ are satisfied. Then, as k varies and passes through the critical value $k = \frac{a(c+d)(d-a)}{m(a+d)}$, system (1.2) undergoes a Hopf bifurcation at $O(0, 0, 0, 0)$.

Proof. Assume that system (1.2) has a pure imaginary root $\lambda = i\omega$, ($\omega \in \mathbb{R}^+$). From (2.1), we get

$$(a - d)\omega^2 - 2akm = 0, \omega^3 - (km - ac - ad)\omega = 0,$$

then

$$\omega = \omega_0 = \sqrt{km - ac - ad}, k = k_0 = \frac{a(c + d)(d - a)}{m(a + d)}.$$

Substituting $k = k_0$ into (2.1), we have

$$\lambda_1 = i\omega_0, \lambda_2 = -i\omega_0, \lambda_3 = d - a, \lambda_4 = -b.$$

Therefore, when $a-d > 0$, $c-d < 0$ and $k = k_0$, the first condition for Hopf bifurcation [24] is satisfied. From (2.1), we have

$$\operatorname{Re}(\lambda'(k_0))|_{\lambda=i\omega_0} = \frac{m(a+d)^2}{2(a+d)(a-d)^2 - 4a^2(c+d)} > 0.$$

Thus, the second condition for a Hopf bifurcation [24] is also met. Hence, Hopf bifurcation exists. \square

Remark 3.1. When $km - ac - ad \leq 0$, system (1.2) has no Hopf bifurcation at the zero equilibrium point.

Theorem 3.2. When $a > d$ and $c + d < 0$, the periodic solutions of (1.2) from Hopf bifurcation at $O(0, 0, 0, 0)$ exist for sufficiently small $0 < |k - k_0| = |k - \frac{a(c+d)(d-a)}{m(a+d)}|$. And the periodic solutions have the following properties:

(I) if $\frac{\delta_2}{\delta_1} > 0$ (resp., $\frac{\delta_2}{\delta_1} < 0$), then the Hopf bifurcation of system (1.2) at $(0, 0, 0, 0)$ is non-degenerate and supercritical (resp. subcritical), and the bifurcating periodic solution exists for $k < k_0$ (resp., $k > k_0$) and is stable (resp., unstable), where

$$\delta_1 = -b \sqrt{-\frac{a^2(c+d)}{a+d}} (a^3 - a^2d + 2acd + ad^2 + d^3)(a+d)(8a^2c + 8a^2d - b^2a - b^2d),$$

$$\begin{aligned} \delta_2 = & (16c + 16d)a^5 + (2bce + 2bde + 16cde + 16d^2e - 3b^2 + 4bc + 4bd)a^4 + (b^2ce - 2b^2de \\ & - 4bc^2e - 6bcde - 2bd^2e - 16c^2de - 32cd^2e - 16d^3e - 3b^2d + 4bcd + 4bd^2 - 16cd^2 - 16d^3)a^3 \\ & + (-2b^2c^2e + 2b^2cde + b^2d^2e + 2bcd^2e + 2bd^3e + 16c^2d^2e + 16cd^3e - 2b^2cd + b^2d^2)a^2 \\ & + (-2b^2c^2de - 3b^2cd^2e + 2b^2d^3e - 4bc^2d^2e - 6bcd^3e - 2bd^4e - 2b^2cd^2 + b^2d^3)a - 4b^2cd^3e - b^2d^4e; \end{aligned}$$

(II) the period and characteristic exponent of the bifurcating periodic solution are

$$T = \frac{2\pi}{\omega_0}(1 + \tau_2\varepsilon^2 + O(\varepsilon^4)), \quad \beta = \beta_2\varepsilon^2 + O(\varepsilon^4),$$

where

$$\varepsilon = \frac{k - k_0}{\mu_2} + O[(k - k_0)^2], \quad \beta_2 = \frac{a^4}{4\delta_1} \left[-2 \sqrt{-\frac{a^2(c+d)}{a+d}} (c+d)\delta_2 \right],$$

$$\tau_2 = \frac{\delta_2 a^3}{4\delta_1(a+d)} \left[\sqrt{2} \sqrt{-\frac{a^2(c+d)}{a+d}} (a^2 - ac - ad - d^2) + a^2c + a^2d + acd + ad^2 \right],$$

$$\mu_2 = \frac{a^4}{4m\delta_1(a+d)^2} \sqrt{-\frac{a^2(c+d)}{a+d}} (c+d)\delta_2 [2(a+d)(a-d)^2 - 4a^2(c+d)];$$

(III) the expression of the bifurcating periodic solution is

$$\begin{bmatrix} u \\ v \\ w \\ p \end{bmatrix} = \begin{bmatrix} \varepsilon a \sqrt{-\frac{2a^2(c+d)}{a+d}} \cos\left(\frac{2\pi t}{T}\right) \\ \varepsilon \left[a \sqrt{-\frac{2a^2(c+d)}{a+d}} \cos\left(\frac{2\pi t}{T}\right) + \frac{2a^2(c+d)}{a+d} \sin\left(\frac{2\pi t}{T}\right) \right] \\ \varepsilon^2 L \\ \varepsilon \frac{a(c+d)(-d+a)}{m(a+d)} \left[\sqrt{-\frac{2a^2(c+d)}{a+d}} \cos\left(\frac{2\pi t}{T}\right) + 2a \sin\left(\frac{2\pi t}{T}\right) \right] \end{bmatrix} + O(\varepsilon^3),$$

where

$$L = -\frac{a^4(c+d)}{ab+bd} + \delta_4[2\cos^2(\frac{2\pi t}{T}) - 1] - \delta_5\sin(\frac{4\pi t}{T}),$$

$$\delta_4 = \frac{a^3(c+d)(4a^2c + 4a^2d - a^2b - adb)}{(a+d)(b^2a + b^2d - 8a^2c - 8a^2d)}, \quad \delta_5 = \frac{a^3(c+d)(2a-b)(a+d)\sqrt{-\frac{2a^2(c+d)}{a+d}}}{(a+d)(b^2a + b^2d - 8a^2c - 8a^2d)}.$$

Proof. Let $k = k_0$, by straightforward computations, we can obtain

$$t_1 = \begin{bmatrix} a\omega_0 \\ a\omega_0 + (k_0m - ac - ad)i \\ 0 \\ 2ak_0i - k_0\omega_0 \end{bmatrix}, \quad t_3 = \begin{bmatrix} 0 \\ 0 \\ 1 \\ 0 \end{bmatrix}, \quad t_4 = \begin{bmatrix} ad - a^2 \\ d^2 - ad \\ 0 \\ k_0(a+d) \end{bmatrix},$$

which satisfy

$$Jt_1 = i\omega_0t_1, \quad Jt_3 = -bt_3, \quad Jt_4 = (d-a)t_4,$$

where

$$J = \begin{bmatrix} -a & a & 0 & 0 \\ c & d & 0 & m \\ 0 & 0 & -b & 0 \\ -k & -k & 0 & 0 \end{bmatrix}.$$

Now, we use transformation $X = QX_1$, where

$$X = (u, v, w, p)^T, \quad X_1 = (u_1, v_1, w_1, p_1)^T,$$

and

$$Q = \begin{bmatrix} aw & 0 & 0 & -a^2 + ad \\ aw & ac + ad - k_0m & 0 & -ad + d^2 \\ 0 & 0 & 1 & 0 \\ -k_0w & -2ak_0 & 0 & k_0(a+d) \end{bmatrix},$$

then, system (1.2) is transformed into

$$\begin{cases} \dot{u}_1 = -\omega_0v_1 + F_1(u_1, v_1, w_1, p_1), \\ \dot{v}_1 = \omega_0u_1 + F_2(u_1, v_1, w_1, p_1), \\ \dot{w}_1 = -bw_1 + F_3(u_1, v_1, w_1, p_1), \\ \dot{p}_1 = -(a-d)p_1 + F_4(u_1, v_1, w_1, p_1), \end{cases} \tag{3.1}$$

where

$$F_1(u_1, v_1, w_1, p_1) = -\frac{w_1}{a\sqrt{-\frac{2a^2(c+d)}{a+d}}(a^3 - a^2d + 2acd + ad^2 + d^3)} \left[\sqrt{-\frac{2a^2(c+d)}{a+d}} a(a+d)(a^2 - ace - d^2e - ad)u_1 - 2a^2e(c+d)(ac + d^2)v_1 - p_1(a-d)(a+d)(a^3 - acde - d^3e - a^2d) \right],$$

$$F_2(u_1, v_1, w_1, p_1) = -\frac{w_1}{2a^2(a^3 - a^2d + 2acd + ad^2 + d^3)} \left[\sqrt{-\frac{2a^2(c+d)}{a+d}} a(a+d)(a^2e + d^2e + 2ad)u_1 + 2ea^2(a^2 + d^2)(c+d)v_1 - dp_1(a-d)(a+d)(a^2e + d^2e + 2a^2) \right],$$

$$F_3(u_1, v_1, w_1, p_1) = \frac{a}{a+d} \left(\sqrt{-\frac{2a^2(c+d)}{a+d}} u_1 - p_1a + dp_1 \right) \left[au_1(a+d) \sqrt{-\frac{2a^2(c+d)}{a+d}} + 2a^2v_1c - a^2dp_1 + 2a^2v_1d + d^3p_1 \right],$$

$$F_4(u_1, v_1, w_1, p_1) = -\frac{w_1}{(a+d)[a^3 + d^3 - ad(a-d-2c)]} \left[\sqrt{-\frac{2a^2(c+d)}{a+d}} a(a+d)(ae - ce + a+d)u_1 + 2a^2e(c+d)(a-c)v_1 - p_1(a-d)(a+d)(ade - cde + a^2 + ad) \right].$$

Furthermore,

$$g_{11} = \frac{1}{4} \left[\frac{\partial^2 F_1}{\partial u_1^2} + \frac{\partial^2 F_1}{\partial v_1^2} + i \left(\frac{\partial^2 F_2}{\partial u_1^2} + \frac{\partial^2 F_2}{\partial v_1^2} \right) \right] = 0,$$

$$g_{02} = \frac{1}{4} \left[\frac{\partial^2 F_1}{\partial u_1^2} - \frac{\partial^2 F_1}{\partial v_1^2} - \frac{2\partial^2 F_2}{\partial u_1 \partial v_1} + i \left(\frac{\partial^2 F_2}{\partial u_1^2} - \frac{\partial^2 F_2}{\partial v_1^2} + \frac{2\partial^2 F_1}{\partial u_1 \partial v_1} \right) \right] = 0,$$

$$g_{20} = \frac{1}{4} \left[\frac{\partial^2 F_1}{\partial u_1^2} - \frac{\partial^2 F_1}{\partial v_1^2} + \frac{2\partial^2 F_2}{\partial u_1 \partial v_1} + i \left(\frac{\partial^2 F_2}{\partial u_1^2} - \frac{\partial^2 F_2}{\partial v_1^2} - \frac{2\partial^2 F_1}{\partial u_1 \partial v_1} \right) \right] = 0,$$

$$G_{21} = \frac{1}{8} \left[\frac{\partial^3 F_1}{\partial u_1^3} + \frac{\partial^3 F_2}{\partial v_1^3} + \frac{\partial^3 F_1}{\partial u_1 \partial v_1^2} + \frac{\partial^3 F_2}{\partial u_1^2 \partial v_1} + i \left(\frac{\partial^3 F_2}{\partial u_1^3} - \frac{\partial^3 F_2}{\partial v_1^3} + \frac{\partial^3 F_2}{\partial u_1 \partial v_1^2} - \frac{\partial^3 F_1}{\partial u_1^2 \partial v_1} \right) \right] = 0.$$

By solving the following equations

$$\begin{bmatrix} -b & 0 \\ 0 & -(a-d) \end{bmatrix} \begin{bmatrix} \omega_{11}^1 \\ \omega_{11}^2 \end{bmatrix} = - \begin{bmatrix} h_{11}^1 \\ h_{11}^2 \end{bmatrix},$$

$$\begin{bmatrix} -b - 2i\omega_0 & 0 \\ 0 & -(a-d) - 2i\omega_0 \end{bmatrix} \begin{bmatrix} \omega_{20}^1 \\ \omega_{20}^2 \end{bmatrix} = - \begin{bmatrix} h_{20}^1 \\ h_{20}^2 \end{bmatrix},$$

where

$$h_{11}^1 = -\frac{a^4(c+d)}{a+d},$$

$$h_{11}^2 = \frac{1}{4} \left(\frac{\partial^2 F_4}{\partial x_1^2} + \frac{\partial^2 F_4}{\partial y_1^2} \right) = 0,$$

$$h_{20}^1 = -a^4(c+d) - ia^3(c+d) \sqrt{-\frac{2a^2(c+d)}{a+d}},$$

$$h_{20}^2 = \frac{1}{4} \left(\frac{\partial^2 F_4}{\partial x_1^2} - \frac{\partial^2 F_4}{\partial y_1^2} - 2i \frac{\partial^2 F_4}{\partial x_1 \partial y_1} \right) = 0,$$

one obtains

$$\omega_{11}^1 = -\frac{a^4(c+d)}{ab+bd}, \quad \omega_{11}^2 = 0, \quad \omega_{20}^2 = 0,$$

$$\begin{aligned}\omega_{20}^1 &= \frac{a^3(c+d)}{(a+d)(b^2a+b^2d-8a^2c-8a^2d)}[4a^2c+4a^2d-a^2b-adb \\ &\quad + i\sqrt{-\frac{2a^2(c+d)}{a+d}}(2a-b)(a+d)], \\ G_{110}^1 &= \frac{1}{2}\left[\left(\frac{\partial^2 F_1}{\partial u_1 \partial w_1} + \frac{\partial^2 F_2}{\partial v_1 \partial w_1}\right) + i\left(\frac{\partial^2 F_2}{\partial u_1 \partial w_1} - \frac{\partial^2 F_1}{\partial v_1 \partial w_1}\right)\right] \\ &= -\frac{1}{4\sqrt{-\frac{a^2(c+d)}{a+d}}(a^3-a^2d+2acd+ad^2+d^3)}\left[2\sqrt{-\frac{a^2(c+d)}{a+d}}\right. \\ &\quad \left.(a-d)(ade-cde+a^2+ad) - i\sqrt{2}(a^2e-2ace-d^2e+2ad)a(c+d)\right], \\ G_{110}^2 &= \frac{1}{2}\left[\left(\frac{\partial^2 F_1}{\partial u_1 \partial p_1} + \frac{\partial^2 F_2}{\partial v_1 \partial p_1}\right) + i\left(\frac{\partial^2 F_2}{\partial u_1 \partial p_1} - \frac{\partial^2 F_1}{\partial v_1 \partial p_1}\right)\right] = 0, \\ G_{101}^1 &= -\frac{1}{4\sqrt{-\frac{a^2(c+d)}{a+d}}(a^3-a^2d+2acd+ad^2+d^3)}\left[2\sqrt{-\frac{a^2(c+d)}{a+d}}(-2a^2ce-a^2de-acde\right. \\ &\quad \left.-ad^2e-cd^2e-2d^3e+a^3-ad^2) - i\sqrt{2}(a^2e+2ace+3d^2e+2ad)a(c+d)\right], \\ G_{101}^2 &= \frac{1}{2}\left[\left(\frac{\partial^2 F_1}{\partial u_1 \partial p_1} - \frac{\partial^2 F_2}{\partial v_1 \partial p_1}\right) + i\left(\frac{\partial^2 F_2}{\partial u_1 \partial p_1} + \frac{\partial^2 F_1}{\partial v_1 \partial p_1}\right)\right] = 0, \\ g_{21} &= G_{21} + \sum_{j=1}^2(2G_{110}^j\omega_{11}^j + G_{101}^j\omega_{20}^j) = \frac{a^4}{4\delta_1}\left[-2\sqrt{-\frac{a^2(c+d)}{a+d}}(c+d)\delta_2 + i\sqrt{2}a(c+d)^2\delta_3\right],\end{aligned}$$

where

$$\delta_1 = -b\sqrt{-\frac{a^2(c+d)}{a+d}}(a^3-a^2d+2acd+ad^2+d^3)(a+d)(8a^2c+8a^2d-b^2a-b^2d),$$

$$\begin{aligned}\delta_2 &= (16c+16d)a^5 + (2bce+2bde+16cde+16d^2e-3b^2+4bc+4bd)a^4 + (b^2ce-2b^2de \\ &\quad -4bc^2e-6bcde-2bd^2e-16c^2de-32cd^2e-16d^3e-3b^2d+4bcd+4bd^2-16cd^2-16d^3)a^3 \\ &\quad + (-2b^2c^2e+2b^2cde+b^2d^2e+2bcd^2e+2bd^3e+16c^2d^2e+16cd^3e-2b^2cd+b^2d^2)a^2 \\ &\quad + (-2b^2c^2de-3b^2cd^2e+2b^2d^3e-4bc^2d^2e-6bcd^3e-2bd^4e-2b^2cd^2+b^2d^3)a-4b^2cd^3e-b^2d^4e,\end{aligned}$$

$$\begin{aligned}\delta_3 &= (16ce+16de+4b)a^4 + (-3b^2e-4bce-32c^2e-32cde-2b^2+32cd+32d^2)a^3 + (6b^2ce \\ &\quad -b^2de+8bc^2e+4bcde-4bd^2e-16cd^2e-16d^3e-6b^2d+8bcd+4bd^2)a^2 + (4b^2cde+b^2d^2e \\ &\quad +8bcd^2e+4bd^3e-4b^2d^2)a+2b^2cd^2e+3b^2d^3e.\end{aligned}$$

Based on above calculation and analysis, we get

$$C_1(0) = \frac{i}{2\omega_0}(g_{20}g_{11} - 2|g_{11}|^2 - \frac{1}{3}|g_{02}|^2) + \frac{1}{2}g_{21} = \frac{1}{2}g_{21},$$

$$\mu_2 = -\frac{\operatorname{Re}C_1(0)}{\alpha'(0)} = \frac{a^4}{4m\delta_1(a+d)^2}\sqrt{-\frac{a^2(c+d)}{a+d}}(c+d)\delta_2[2(a+d)(a-d)^2-4a^2(c+d)],$$

$$\tau_2 = \frac{\delta_2 a^3}{4\delta_1(a+d)} \left[\sqrt{2} \sqrt{-\frac{a^2(c+d)}{a+d}} (a^2 - ac - ad - d^2) + a^2c + a^2d + acd + ad^2 \right],$$

where

$$\omega'(0) = -\frac{1}{2} \sqrt{-\frac{a^2(c+d)}{a+d}} \frac{(a^2 - ac - ad - d^2)(a+d) \sqrt{2}m}{a(a^3c + a^3d - 2a^2c^2 - 5a^2cd - 3a^2d^2 - acd^2 - ad^3 + cd^3 + d^4)},$$

$$\alpha'(0) = \frac{m(a+d)^2}{2(a+d)(a-d)^2 - 4a^2(c+d)},$$

$$\beta_2 = 2\text{Re}C_1(0) = \frac{a^4}{4\delta_1} \left[-2 \sqrt{-\frac{a^2(c+d)}{a+d}} (c+d)\delta_2 \right].$$

From $a - d > 0$ and $c + d < 0$, we have if $\frac{\delta_2}{\delta_1} > 0$ (resp., $\frac{\delta_2}{\delta_1} < 0$), then $\mu_2 < 0$ (resp., $\mu_2 > 0$) and $\beta_2 > 0$ (resp., $\beta_2 < 0$), the Hopf bifurcation of system (1.2) at $(0, 0, 0, 0)$ is non-degenerate and supercritical (resp. subcritical), and the bifurcating periodic solution exists for $k < k_0$ (resp., $k > k_0$) and is stable (resp., unstable).

Furthermore, the period and characteristic exponent are

$$T = \frac{2\pi}{\omega_0} (1 + \tau_2 \varepsilon^2 + O(\varepsilon^4)), \quad \beta = \beta_2 \varepsilon^2 + O(\varepsilon^4),$$

where $\varepsilon = \frac{k-k_0}{\mu_2} + O[(k - k_0)^2]$.

And the expression of the bifurcating periodic solution is (except for an arbitrary phase angle)

$$X = (u, v, w, p)^T = Q(\bar{y}_1, \bar{y}_2, \bar{y}_3, \bar{y}_4)^T = QY,$$

where

$$\begin{aligned} \bar{y}_1 &= \text{Re}\mu, \quad \bar{y}_2 = \text{Im}\mu, \quad (\bar{y}_3, \bar{y}_4)^T = \omega_{11}|\mu|^2 + \text{Re}(\omega_{20}\mu^2) + O(|\mu|^2), \\ \omega_{11} &= (\omega_{11}^1, 0)^T, \quad \omega_{20} = (\omega_{20}^1, 0)^T, \end{aligned}$$

and

$$\mu = \varepsilon e^{\frac{2i\pi t}{T}} + \frac{i\varepsilon^2}{6\omega_0} [g_{02}e^{-\frac{4i\pi t}{T}} - 3g_{20}e^{\frac{4i\pi t}{T}} + 6g_{11}] + O(\varepsilon^3) = \varepsilon e^{\frac{2i\pi t}{T}} + O(\varepsilon^3).$$

By computations, we can obtain

$$\begin{bmatrix} u \\ v \\ w \\ p \end{bmatrix} = \begin{bmatrix} \varepsilon a \sqrt{-\frac{2a^2(c+d)}{a+d}} \cos\left(\frac{2\pi t}{T}\right) \\ \varepsilon \left[a \sqrt{-\frac{2a^2(c+d)}{a+d}} \cos\left(\frac{2\pi t}{T}\right) + \frac{2a^2(c+d)}{a+d} \sin\left(\frac{2\pi t}{T}\right) \right] \\ \varepsilon^2 L \\ \varepsilon \frac{a(c+d)(-d+a)}{m(a+d)} \left[\sqrt{-\frac{2a^2(c+d)}{a+d}} \cos\left(\frac{2\pi t}{T}\right) + 2a \sin\left(\frac{2\pi t}{T}\right) \right] \end{bmatrix} + O(\varepsilon^3),$$

where

$$L = -\frac{a^4(c+d)}{ab+bd} + \delta_4 \left[2\cos^2\left(\frac{2\pi t}{T}\right) - 1 \right] - \delta_5 \sin\left(\frac{4\pi t}{T}\right),$$

$$\delta_4 = \frac{a^3(c+d)(4a^2c+4a^2d-a^2b-adb)}{(a+d)(b^2a+b^2d-8a^2c-8a^2d)},$$

$$\delta_5 = \frac{a^3(c+d)(2a-b)(a+d)\sqrt{-\frac{2a^2(c+d)}{a+d}}}{(a+d)(b^2a+b^2d-8a^2c-8a^2d)}.$$

Based on the above discussion, the conclusions of Theorem 3.2 are proved. □

In order to verify the above theoretical analysis, we assume

$$a = 1, \quad b = 0.5, \quad c = -2, \quad d = 0.5, \quad m = 1, \quad e = 1.$$

According to Theorem 3.1, we get $k_0 = 1$. Then from Theorem 3.2, $\mu_2 = -51.111$ and $\beta_2 = 17.037$, which imply that the Hopf bifurcation of system (1.2) at $(0, 0, 0, 0)$ is nondegenerate and supercritical, a bifurcation periodic solution exists for $k < k_0 = 1$ and the bifurcating periodic solution is stable. Figure 11(I) shows the Hopf periodic solution occurs when $k = 0.9999 < k_0 = 1$. Based on above conclusions, in this case, it can be seen that the critical value k_0 and the properties of Hopf bifurcation of system (1.2) at $(0, 0, 0, 0)$ still remain unchanged with the parameters $(a, b, c, d, m, e) = (1, 10, -2, 0.5, 1, 10)$. By computations, we get $\mu_2 = -13.292$ and $\beta_2 = 4.430$. The corresponding Hopf periodic orbit with $k = 0.9999$ is given in Figure 11(II).

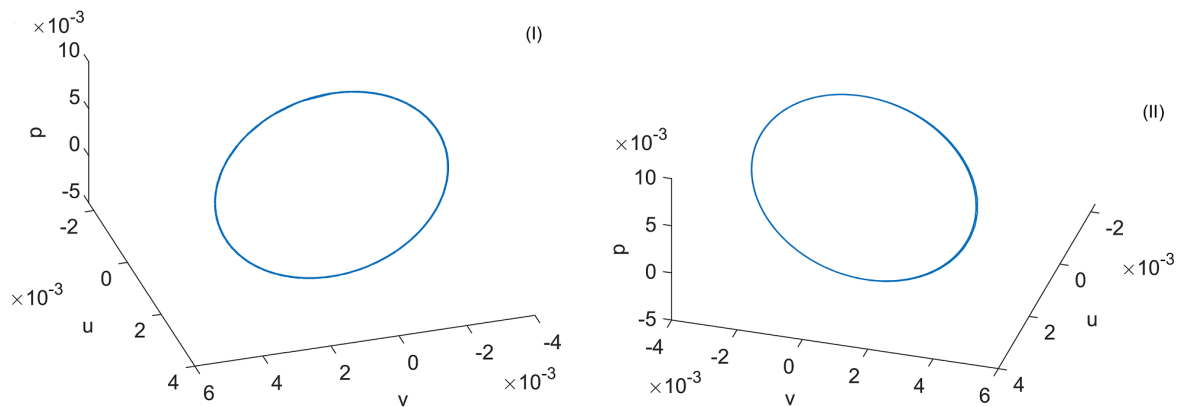


Figure 11. Phase portraits of (1.2) with (I) $(b, e) = (0.5, 1)$, (II) $(b, e) = (10, 10)$.

4. Hyperchaos control

In some cases, chaos usually is harmful and need to be suppressed, such as in pendulum system [25], wind power system [26] and spiral waves chaos [27], etc.. Therefore, chaos control has been widely concerned by scholars, and many valuable hyperchaos control methods have emerged, such as universal adaptive feedback control [28], linear state-feedback control and fuzzy disturbance-observer-based terminal sliding mode control scheme [29,30], etc. In addition, the chaos control can be achieved based on the ultimate boundedness of a chaotic system [31–33]. In this section, we will control hyperchaotic system (1.2) to stable equilibrium $(0, 0, 0, 0)$ by using the linear feedback control method. Suppose that

the controlled hyperchaotic system is given by

$$\begin{cases} \dot{u} = a(v - u) + evw + c_1u, \\ \dot{v} = cu + dv - uw + mp + c_2v, \\ \dot{w} = -bw + uv + c_3w, \\ \dot{p} = -ku - kv + c_4p, \end{cases} \quad (4.1)$$

where c_j ($j = 1, 2, 3, 4$) are feedback coefficients. The Jacobian matrix of system (4.1) at zero equilibrium point is

$$J_c = \begin{bmatrix} -a + c_1 & a & 0 & 0 \\ c & d + c_2 & 0 & m \\ 0 & 0 & -b + c_3 & 0 \\ -k & -k & 0 & c_4 \end{bmatrix}.$$

The characteristic equation of J_c at zero equilibrium point is

$$f(\lambda) = \lambda^4 + t_3\lambda^3 + t_2\lambda^2 + t_1\lambda + t_0,$$

where

$$t_0 = abcc_4 + abdc_4 + 2abkm + abc_2c_4 - acc_3c_4 - adc_3c_4 - 2akmc_3 - ac_2c_3c_4 - bdc_1c_4 - bkmc_1 - bc_1c_2c_4 + dc_1c_3c_4 + kmc_1c_3 + c_1c_2c_3c_4,$$

$$t_1 = (c_3c_4 - bc - bd - bc_2 - bc_4 + cc_3 + cc_4 + dc_3 + dc_4 + 2km + c_3c_2 + c_2c_4)a + (bc_1 + bc_4 - c_1c_3 - c_1c_4 - c_3c_4)d + b(km + c_1c_2 + c_1c_4 + c_2c_4) - (km + c_1c_2 + c_1c_4 + c_2c_4)c_3 - kmc_1 - c_1c_2c_4,$$

$$t_2 = ab - ac - ad - ac_2 - ac_3 - ac_4 - bd - bc_1 - bc_2 - bc_4 + dc_1 + dc_3 + dc_4 + km + c_1c_2 + c_1c_3 + c_1c_4 + c_2c_3 + c_2c_4 + c_3c_4,$$

$$t_3 = a + b - d - c_1 - c_2 - c_3 - c_4.$$

According to Routh-Hurwitz criterion [23], the real parts of eigenvalues are negative if and only if

$$t_3(t_1t_2 - t_3t_0) - t_1^2 > 0, \quad t_3t_2 - t_1 > 0, \quad t_3 > 0, \quad t_0 > 0. \quad (4.2)$$

Case 1. For the parameters $a = 15$, $b = 43$, $c = 1$, $d = 16$, $e = 5$, $m = 5$, $k = 2$, we assume $c_j = -20$ ($j = 1, 2, 3, 4$), system (4.1) has only one equilibrium point $(0, 0, 0, 0)$, and the corresponding eigenvalues are

$$\lambda_1 = -63, \quad \lambda_2 = -4.468, \quad \lambda_3 = -35.756, \quad \lambda_4 = -18.774,$$

the equilibrium point is asymptotically stable.

Case 2. For the parameters $b = 43$, $a = 15$, $c = 1$, $e = 5$, $k = 5$, $d = 16$, $m = 0.5$, we assume $c_j = -20$ ($j = 1, 2, 3, 4$), system (4.1) also has only one equilibrium point $(0, 0, 0, 0)$, and the corresponding eigenvalues are

$$\lambda_1 = -63, \quad \lambda_2 = -3.747, \quad \lambda_3 = -19.703, \quad \lambda_4 = -35.549,$$

the zero equilibrium point is asymptotically stable.

For the two cases, the behaviors of the state (u, v, w, p) of hyperchaotic system (1.2) and controlled hyperchaotic system (4.1) with time are shown in Figures 12 and 13, respectively. These indicate that

the controlled hyperchaotic system (4.1) is asymptotically stable at zero-equilibrium point by selecting appropriate feedback coefficients.

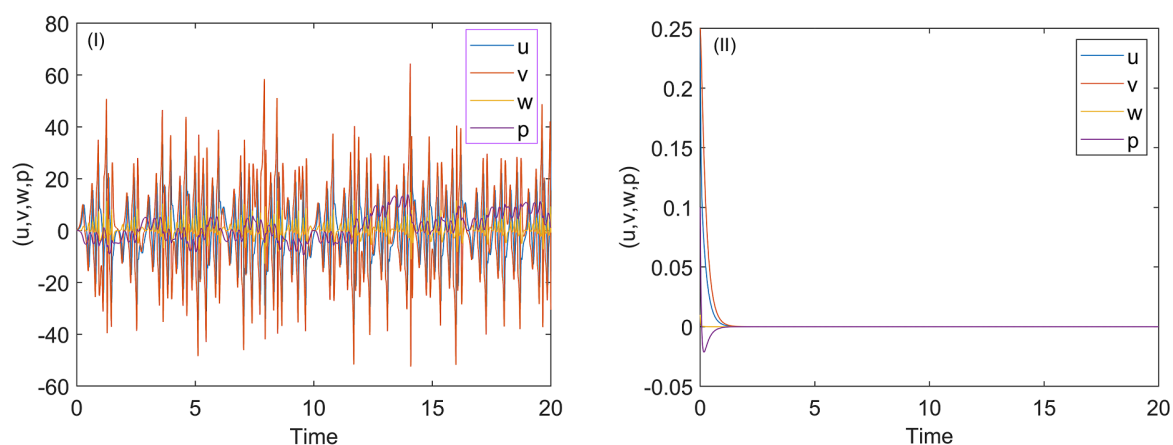


Figure 12. Time series of (I) system (1.2), (II) system (4.1) (Case 1).

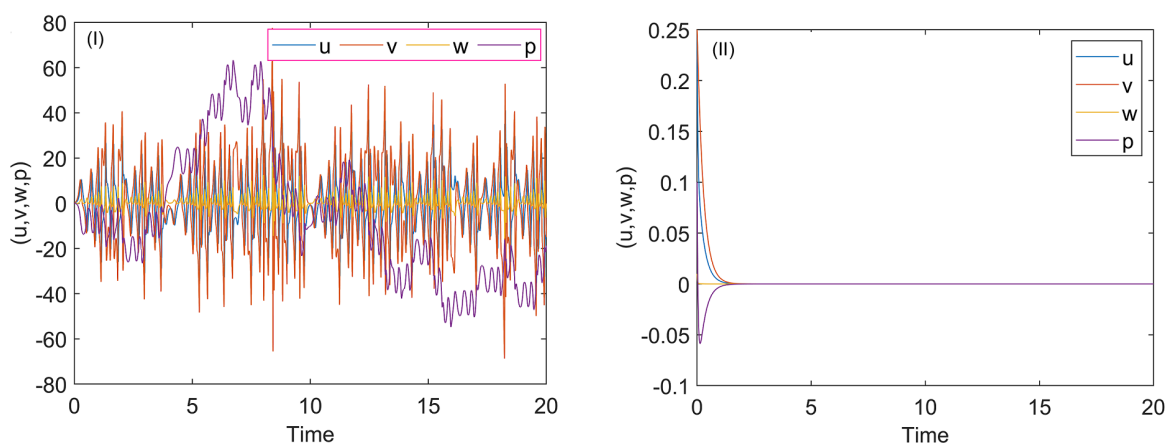


Figure 13. Time series of (I) system (1.2), (II) system (4.1) (Case 2).

5. Conclusions

In this paper, we present a new 4D hyperchaotic system by introducing a linear controller to the second equation of the 3D chaotic Qi system. The new system always has two unstable nonzero equilibrium points which are symmetric about w axis. The complex dynamical behaviors, including dissipativity and invariance, equilibria and their stability, quasi-periodicity, chaos and hyperchaos of new 4D system (1.2) are investigated and analyzed. Furthermore, the existence of Hopf bifurcation, the stability and expression of the Hopf bifurcation at zero-equilibrium point are studied using the normal form theory and symbolic computations. Based on Section 3, it can also be seen that the parameters b and e are unrelated to the critical value k of Hopf bifurcation of the new 4D system. In order to analyze and verify the complex phenomena of the system, some numerical simulations are carried out including Lyapunov exponents, bifurcation and Poincaré maps, etc. The results show that the new 4D hyperchaotic system can exhibit complex dynamical behaviors, such as quasi-periodic, chaotic and hyperchaotic. Furthermore, the resistors, capacitors, operational amplifiers and analog multipliers

can be used to design the hyperchaotic electronic circuit, to verify the existence of the hyperchaotic attractor of the system from another perspective, embodying the application of the hyperchaotic circuit system. We will investigate the ultimate bound sets of the hyperchaotic system, a new method for hyperchaos control and hyperchaotic electronic circuit in a future study.

Acknowledgments

Project supported by the Doctoral Scientific Research Foundation of Hanshan Normal University (No. QD202130).

Conflict of interest

The authors declare that they have no conflict of interest.

References

1. O. Rössler, An equation for hyperchaos, *Phys. Lett. A*, **71** (1979), 155–157. [https://doi.org/10.1016/0375-9601\(79\)90150-6](https://doi.org/10.1016/0375-9601(79)90150-6)
2. S. Zhang, T. Gao, A coding and substitution frame based on hyper-chaotic systems for secure communication, *Nonlinear Dyn.*, **84** (2016), 833–849. <https://doi.org/10.1007/s11071-015-2530-2>
3. H. Li, Z. Hua, H. Bao, L. Zhu, M. Chen, B. Bao, Two-dimensional memristive hyperchaotic maps and application in secure communication, *IEEE T. Ind. Electron.*, **68** (2021), 9931–9940. <https://doi.org/10.1109/TIE.2020.3022539>
4. Q. Li, H. Zeng, J. Li, Hyperchaos in a 4D memristive circuit with infinitely many stable equilibria, *Nonlinear Dyn.*, **79** (2015), 2295–2308. <https://doi.org/10.1007/s11071-014-1812-4>
5. Z. Wang, F. Min, E. Wang, A new hyperchaotic circuit with two memristors and its application in image encryption, *AIP Adv.*, **6** (2016), 095316. <https://doi.org/10.1063/1.4963743>
6. N. Fataf, S. Palit, S. Mukherjee, M. Said, D. Son, S. Banerjee, Communication scheme using a hyperchaotic semiconductor laser model: chaos shift key revisited, *Eur. Phys. J. Plus*, **132** (2017), 492. <https://doi.org/10.1140/epjp/i2017-11786-y>
7. E. Barakat, M. Abdel-Aty, I. El-Kalla, Hyperchaotic and quasiperiodic behaviors of a two-photon laser with multi-intermediate states, *Chaos Soliton. Fract.*, **152** (2021), 111316. <https://doi.org/10.1016/j.chaos.2021.111316>
8. Q. Jia, Projective synchronization of a new hyperchaotic Lorenz system, *Phys. Lett. A*, **370** (2007), 40–45. <https://doi.org/10.1016/j.physleta.2007.05.028>
9. Y. Chen, Q. Yang, Dynamics of a hyperchaotic Lorenz-type system, *Nonlinear Dyn.*, **77** (2014), 569–581. <https://doi.org/10.1007/s11071-014-1318-0>
10. J. Singh, B. Roy, Hidden attractors in a new complex generalised Lorenz hyperchaotic system, its synchronisation using adaptive contraction theory, circuit validation and application, *Nonlinear Dyn.*, **92** (2018), 373–394. <https://doi.org/10.1007/s11071-018-4062-z>

11. Q. Lai, Z. Wan, P. Kuate, H. Fotsin, Dynamical analysis, circuit implementation and synchronization of a new memristive hyperchaotic system with coexisting attractors, *Mod. Phys. Lett. B*, **35** (2021), 2150187. <https://doi.org/10.1142/S0217984921501876>
12. K. Thamilaran, M. Lakshmanan, A. Venkatesan, Hyperchaos in a modified canonical chua's circuit, *Int. J. Bifurcat. Chaos*, **14** (2004), 221–243. <https://doi.org/10.1142/S0218127404009119>
13. M. Sahin, A. Demirkol, H. Guler, S. Hamamci, Design of a hyperchaotic memristive circuit based on wien bridge oscillator, *Comput. Electr. Eng.*, **88** (2020), 106826. <https://doi.org/10.1016/j.compeleceng.2020.106826>
14. M. Abdul Rahim, H. Natiq, N. Fataf, S. Banerjee, Dynamics of a new hyperchaotic system and multistability, *Eur. Phys. J. Plus*, **134** (2019), 499. <https://doi.org/10.1140/epjp/i2019-13005-5>
15. H. Natiq, S. Banerjee, S. He, M. Said, A. Kilicman, Designing an M-dimensional nonlinear model for producing hyperchaos, *Chaos Soltion. Fract.*, **114** (2018), 506–515. <https://doi.org/10.1016/j.chaos.2018.08.005>
16. G. Qi, B. Wyk, M. Wyk, A four-wing attractor and its analysis, *Chaos Soliton. Fract.*, **40** (2009), 2016–2030. <https://doi.org/10.1016/j.chaos.2007.09.095>
17. G. Qi, X. Liang, Mechanical analysis of Qi four-wing chaotic system, *Nonlinear Dyn.*, **86** (2016), 1095–1106. <https://doi.org/10.1007/s11071-016-2949-0>
18. C. Xu, Q. Zhang, On the chaos control of the Qi system, *J. Eng. Math.*, **90** (2015), 67–81. <https://doi.org/10.1007/s10665-014-9730-5>
19. G. Qi, J. Zhang, Energy cycle and bound of Qi chaotic system, *Chaos Soliton. Fract.*, **99** (2017), 7–15. <https://doi.org/10.1016/j.chaos.2017.03.044>
20. X. Wang, Y. Zhang, Y. Gao, Hyperchaos generated from Qi system and its observer, *Mod. Phys. Lett. B*, **23** (2009), 963–974. <https://doi.org/10.1142/S021798490901920X>
21. X. Wang, Y. Gao, Y. Zhang, Hyperchaos Qi system, *Int. J. Mod. Phys. B*, **24** (2010), 4771–4778. <https://doi.org/10.1142/S0217979210055895>
22. K. Sudheer, M. Sabir, Switched modified function projective synchronization of hyperchaotic Qi system with uncertain parameters, *Commun. Nonlinear Sci.*, **15** (2010), 4058–4064. <https://doi.org/10.1016/j.cnsns.2010.01.014>
23. E. De Jesus, C. Kaufman, Routh-Hurwitz criterion in the examination of eigenvalues of a system of nonlinear ordinary differential equations, *Phys. Rev. A*, **35** (1987), 5288. <https://doi.org/10.1103/PhysRevA.35.5288>
24. J. Guckenheimer, P. Holmes, *Nonlinear oscillations, dynamical systems and bifurcations of vector fields*, New York: Springer, 1983. <https://doi.org/10.1007/978-1-4612-1140-2>
25. X. Chen, Z. Jing, X. Fu, Chaos control in a pendulum system with excitations and phase shift, *Nonlinear Dyn.*, **78** (2014), 317–327. <https://doi.org/10.1007/s11071-014-1441-y>
26. C. Wang, H. Zhang, W. Fan, P. Ma, Finite-time function projective synchronization control method for chaotic wind power systems, *Chaos Soliton. Fract.*, **135** (2020), 109756. <https://doi.org/10.1016/j.chaos.2020.109756>
27. G. Yuan, S. Chen, S. Yang, Eliminating spiral waves and spatiotemporal chaos using feedback signal, *Eur. Phys. J. B*, **58** (2007), 331–336. <https://doi.org/10.1140/epjb/e2007-00220-6>

28. J. Zheng, A simple universal adaptive feedback controller for chaos and hyperchaos control, *Comput. Math. Appl.*, **61** (2011), 2000–2004. <https://doi.org/10.1016/j.camwa.2010.08.050>
29. S. Sajjadi, D. Baleanu, A. Jajarmi, H. Pirouz, A new adaptive synchronization and hyperchaos control of a biological snap oscillator, *Chaos Soliton. Fract.*, **138** (2020), 109919. <https://doi.org/10.1016/j.chaos.2020.109919>
30. H. Jahanshahi, A. Yousefpour, Z. Wei, R. Alcaraz, S. Bekiros, A financial hyperchaotic system with coexisting attractors: dynamic investigation, entropy analysis, control and synchronization, *Chaos Soliton. Fract.*, **126** (2019), 66–77. <https://doi.org/10.1016/j.chaos.2019.05.023>
31. F. Chien, A. Roy Chowdhury, H. Saberi Nik, Competitive modes and estimation of ultimate bound sets for a chaotic dynamical financial system, *Nonlinear Dyn.*, **106** (2021), 3601–3614. <https://doi.org/10.1007/s11071-021-06945-8>
32. H. Saberi Nik, S. Effati, J. Saberi-Nadjafi, New ultimate bound sets and exponential finite-time synchronization for the complex Lorenz system, *J. Complexity*, **31** (2015), 715–730. <https://doi.org/10.1016/j.jco.2015.03.001>
33. M. Zahedi, H. Saberi Nik, Bounds of the chaotic system for couette-Taylor flow and its application in finite-time control, *Int. J. Bifurcat. Chaos*, **25** (2015), 1550133. <https://doi.org/10.1142/S0218127415501333>



AIMS Press

©2023 the Author(s), licensee AIMS Press. This is an open access article distributed under the terms of the Creative Commons Attribution License (<http://creativecommons.org/licenses/by/4.0>)